Superexchange Coupling and Slow Magnetic Relaxation in a Transuranium Polymetallic Complex

N. Magnani,* E. Colineau, R. Eloirdi, J.-C. Griveau, and R. Caciuffo†
European Commission, Joint Research Centre, Institute for Transuranium Elements, Postfach 2340, D-76125 Karlsruhe, Germany

S. M. Cornet, I. May,‡ and C. A. Sharrad
Centre for Radiochemistry Research, School of Chemistry, The University of Manchester, Oxford Road, Manchester, United Kingdom M13 9PL

D. Collison and R. E. P. Winpenny
School of Chemistry, The University of Manchester, Oxford Road, Manchester, United Kingdom M13 9PL
(Received 8 March 2010; published 11 May 2010)

$\{Np^{VI}O_2Cl_2\}\{Np^{V}O_2Cl(thf)_3\}_2$ is the first studied example of a polymetallic transuranic complex displaying both slow relaxation of the magnetization and effective superexchange interactions between $5f$ centers. The coupling constant for Np^{V}-Np^{VI} pairs is 10.8 K, more than 1 order of magnitude larger than the common values found for rare-earth ions in similar environments. The dynamic magnetic behavior displays slow relaxation of magnetization of molecular origin with an energy barrier of 140 K, which is nearly twice the size of the highest barrier found in polymetallic clusters of the d block. Our observations also suggest that future actinide-based molecular magnets will have very different behavior to lanthanide-based clusters.

DOI: 10.1103/PhysRevLett.104.197202 PACS numbers: 75.50.Xx, 71.70.Ch, 71.70.Gm, 75.30.Et

Polymetallic complexes (often called *clusters*) displaying intramolecular exchange coupling are the subject of intensive research in such diverse fields as quantum information processes, magnetocaloric refrigeration, and spintronic applications [1]. Clusters with energetically isolated high-spin ground state and magnetic bistability, conventionally dubbed as single molecule magnets (SMMs), could lead to the realization of ultrahigh density memory components [2]. The low anisotropy energy barrier typical of transition-metal complexes can be considerably improved by using rare-earth ions [3], but the limited radial extent of the $4f$ shell implies small exchange coupling, so that the synthesis of clusters carrying a large magnetic moment is not realistic. Actinides, whose unfilled $5f$ shell is responsible for peculiar magnetic properties at the boundary between transition metals and rare earths [4], would allow both limitations to be overcome. While a signature of slow magnetic relaxation has recently been observed in monometallic uranium molecules [5], polymetallic actinide complexes displaying superexchange interactions are exceedingly rare [6,7], and the presence of $3d$ metal ions or radical species with unpaired electrons is almost always required to clearly establish the presence of a sizable magnetic coupling [8].

Here we report on a heterovalent Np trimetallic cluster which displays both sizable superexchange between its transuranic centers and slow relaxation of magnetization. The $\{Np^{VI}O_2Cl_2\}\{Np^{V}O_2Cl(thf)_3\}_2$ (hereafter Np_3) trimetallic mixed-oxidation-state cluster studied in the present work is depicted in Fig. 1. Its two Np^{V} ions are linked through two bridging chlorides, their distorted pentagonal bipyramidal inner coordination spheres being completed by three coordinated tetrahydrofuran (thf) molecules per metal center [9]. One neptunyl oxygen from each of the two neptunyl(V) species coordinates into the equatorial plane of a neptunyl(VI) center, which has a distorted tetragonal bipyramidal geometry completed by two coordinated chloride ligands. From the magnetic point of view, the system can be schematized as an isosceles triangle, so that in principle two different superexchange interactions can be present (one between two heterovalent centers, mediated by one oxygen, and another between the two homovalent Np^{V}, mediated by two chlorines).

A 5 mg sample of Np_3 was prepared using the method described in a previous work [9]; dc magnetization measurements were carried out with a Quantum Design SQUID magnetometer in the temperature (T) range from

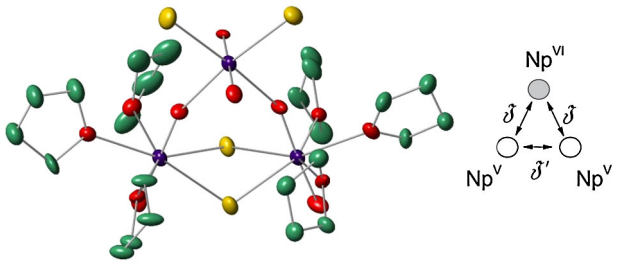

FIG. 1 (color online). Left, structure of the Np_3 cluster studied in the present work (Np blue [dark gray], Cl yellow [light gray], O red [medium-dark gray], C green [medium gray], H not shown for clarity). Right, schematic model of the superexchange interactions.

2 to 300 K and with a magnetic field of up to 7 T. The ratio χ between the longitudinal magnetic moment and the applied field is plotted in Fig. 2 as χT vs T. The raw experimental data were corrected by subtracting the calculated diamagnetic contribution, $\chi_d = -7.3 \times 10^{-4}$ emu/mol, and a temperature-independent magnetization term, $M_d = 5.4 \times 10^{-3}\ \mu_B$, which was systematically detected at zero field in all reference curves. Above 30 K, χ follows a C/T Curie behavior with a C constant of about 1.88 emu K/mol. This result indicates immediately that all three Np centers have a magnetic ground state; in fact, the maximum contribution to C that could be provided by the Np^{VI} Kramers ion is 0.8 emu K/mol, the value corresponding to the free $5f^1$ ion. Moreover, the fact that in this range χT is independent of both the temperature and the applied field value indicates that the ligand field splits the ground-state multiplet of each ion in a group of fully populated low-energy levels well separated from the excited states by an energy gap which does not allow them to become thermally populated; in fact the observed value of the Curie constant C is clearly reduced with respect to the sum of the free-ion contributions. Below 30 K, on the other hand, the low-field χT first increases with decreasing temperature, then abruptly decreases towards zero. In this temperature range, the shape of the curves strongly depends on the applied field value.

The observed magnetic behavior can be understood by considering the combined effects of the ligand field and the

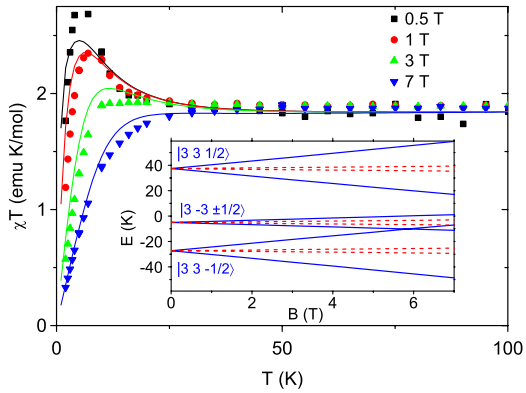

FIG. 2 (color online). Plots of χT vs T for Np_3. Data have been collected with applied field values of 0.5, 1, 3, and 7 T as reported in the legend. Solid lines are the results of calculations assuming ligand-field and superexchange interactions between pairs of Np centers as indicated in Fig. 1. Inset: Calculated energy spectra of the Np_3 cluster as a function of the magnetic field. Dashed red lines are calculated with the magnetic field applied along the direction perpendicular to the plane of the Np_3 triangle, while full blue lines are obtained when the magnetic field is applied within the plane and forms the same angle with the quantization axis of the two Np^V centers. For the latter configurations, the eigenstates can be labeled by the J_z component of each individual Np moment as indicated in the figure (note that changing the sign of all three quantum numbers results in states which are degenerate in absence of an applied magnetic field).

superexchange interactions. The trimetallic cluster can be modeled as an isosceles triangle formed by a $5f^1$ center and the two equivalent $5f^2$ ions, respectively characterized by a $^2F_{5/2}$ and a $^3H_4$ lowest energy multiplet. The appropriate Hamiltonian takes the form

$$H = \sum_{i=1}^{3} H_{\mathrm{LF}}^{(i)} + H_{\mathrm{SE}} + H_Z, \tag{1}$$

where

$$H_{\mathrm{LF}}^{(i)} = \sum_{k=1}^{3} \sum_{q=-2k}^{2k} B_{2k}^{q}(i) O_{2k}^{q}(i) \tag{2}$$

is the ligand-field Hamiltonian acting on the ith ion, $O_{2k}^{q}(i)$ being the Stevens operators equivalents [10] and $B_{2k}^{q}(i)$ the ligand-field parameters;

$$H_{\mathrm{SE}} = \Im \mathbf{J}^{(1)} \cdot (\mathbf{J}^{(2)} + \mathbf{J}^{(3)}) + \Im' \mathbf{J}^{(2)} \cdot \mathbf{J}^{(3)} \tag{3}$$

is the superexchange Hamiltonian, $\mathbf{J}^{(i)}$ is the total angular momentum of the ith ion, $\Im$ and $\Im'$ are the Np^{VI}-Np^V and Np^V-Np^V exchange constants respectively; finally,

$$H_Z = -\mu_B \mathbf{B} \cdot \sum_{i=1}^{3} g_i \mathbf{J}^{(i)} \tag{4}$$

is the Zeeman term describing the effect of the external magnetic field $\mathbf{B}$, g_i being the Landé factor of the ith ion [11]. We remark that, in contrast to the spin-only case of transition-metal clusters, the orbital degrees of freedom for f electrons are not quenched; however, the strong spin-orbit coupling allows us to treat superexchange by an effective Hamiltonian acting on the total angular momentum $\mathbf{J} = \mathbf{L} + \mathbf{S}$. The point symmetry at Np sites is extremely low for this complex; however, ligand-field calculations can be simplified by taking into account the presence of two oxygen ligands at very close distances (between 1.75 and 1.91 Å) around each neptunium, and forming an angle close to 180 degrees. We assume that this defines the local quantization axis for each of the three sites [12] so that, once the noncollinearity between the corresponding magnetic moments is taken into account, the main contributions to the ligand-field Hamiltonians (2) arise from the axial terms ($q = 0$) [10]. A similar model has been invoked to successfully explain the magnetic properties of exchange-coupled Dy-based complexes [13]. In this framework, the ligand-field spectra for a Kramers ion with half-integer total momentum J is composed of several doublets labeled by $J_z = \pm M$ ($M \leq J$), whereas a non-Kramers ion with integer J displays the $M = 0$ nonmagnetic singlet in addition to the above doublets. Table I lists the calculated values of the Curie constant C assuming all the possible well-isolated ground states for the Np^V and Np^{VI} sites of Np_3. The experimental value of C is exactly reproduced assuming the presence of a dominant axial ligand-field term on the Np ions, leading to $J_z = \pm 3$ doublet ground states for the Np^V pair and

TABLE I. Calculated values of the Curie constant C (expressed in emu K/mol) for different combinations of single-ion ground states of the Np_3 trimetallic complex. The experimentally determined value of C above 30 K, where the effects of superexchange are negligible, is 1.88 emu K/mol.

Np^V ground state	Np^{VI} ground state $\lvert\pm\frac{1}{2}\rangle$	$\lvert\pm\frac{3}{2}\rangle$	$\lvert\pm\frac{5}{2}\rangle$
$\lvert 0\rangle$	0.44	0.21	0.57
$\lvert\pm 1\rangle$	0.60	0.37	0.73
$\lvert\pm 2\rangle$	1.08	0.85	1.21
$\lvert\pm 3\rangle$	1.88	1.65	2.02
$\lvert\pm 4\rangle$	3.00	2.77	3.14

isolating a $J_z = \pm\frac{1}{2}$ doublet for the Np^{VI} ion. To confirm the physical likeliness of this choice, the left panel in Fig. 3 shows the possible combinations of the three axial ligand-field parameters which give rise to a $J_z = \pm 3$ ground-state doublet for the two Np^V ($5f^2$) centers. To be physically significant, the variation of the two ratios B_4^0/B_2^0 and B_6^0/B_2^0 is limited within a range of the same order of magnitude as the ratio between the corresponding Stevens factors [14]. Each of the four full black straight lines in the plot is the solution of one equation of the form $E_M = E_3$, where E_M indicates the calculated energy of the corresponding $J_z = \pm M$ state(s), $M = 0, 1, 2, 4$. The light-blue and the light-red zones indicate where the $J_z = \pm 3$ doublet becomes the lowest in energy, the former constraining B_2^0 to be positive and the latter negative. The situation is even simpler for the $5f^1$ electronic configuration of Np^{VI}. In this case, only two axial parameters have to be considered since the sixth-order Stevens factor is nil [14]. As in the previous case, the colored area in the right-hand-side plot of Fig. 3 represents the zone within the parameter space where the $J_z = \pm 1/2$ doublet is the ground state.

The presence of superexchange coupling is evident in the low-temperature interval, where the χT curves are strongly field dependent and deviate from the Curie behavior. The ratio between the magnetization and the applied field has been calculated from the diagonalization of $H_{SE} + H_Z$ projected within the subspace defined by the ligand-field ground states of the complex, and properly averaged to reflect the polycrystalline nature of the sample. This calculation procedure follows directly the definition used to treat the experimental data and keeps into account possible saturation effects, which cannot be ruled out since working with encapsulated samples requires the use of magnetic fields larger than those usually employed in susceptibility measurements. According to the results of this quantitative analysis, shown in Fig. 2, the experimental data can be well reproduced assuming a large coupling $\Im = 10.8$ K between the two pairs of Np ions with different valence, and a significantly weaker interaction $\Im' = 0.56$ K between the two Np^V centers. By numerical diagonalization of Eq. (1) we have checked that these values are not influenced by the actual ligand-field strength, provided that the $J_z = \pm 3$ doublet on the non-Kramers ions is not significantly split by the nonaxial term [15]. This qualitative conclusion does not change if the natural quantization axis of each ion does not exactly coincide with the direction of the two closest oxygen ligands, or if a reasonable mixing of different states with the ground $J_z = \pm 1/2$ doublet of the Np^{VI} ion is allowed; in those cases, the experimental data can still be reproduced using slightly different values of the exchange constants.

Figure 4 shows the ac magnetic susceptibility curves measured as a function of temperature for different frequencies f of the driving magnetic field. The real and imaginary linear components of the ac magnetic susceptibility were measured as a function of temperature with a Quantum Design PPMS-14T system using the mutual-

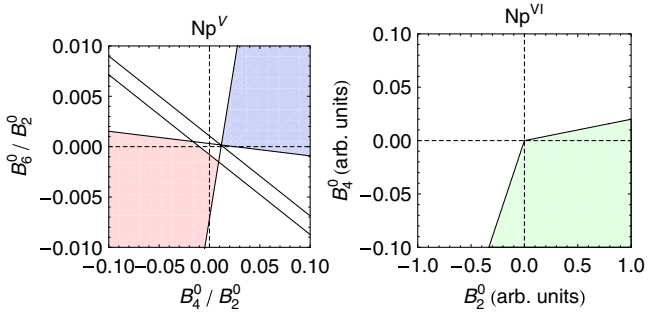

FIG. 3 (color online). Left panel: Np^V ($5f^2$) axial ligand-field parameters regions leading to a $J_z = \pm 3$ ground-state doublet for positive (light-blue zone, containing most of the first quadrant) and negative (light-red zone, containing most of the third quadrant) B_2^0 values. Right panel: Np^{VI} ($5f^1$) axial ligand-field parameters region leading to a $J_z = \pm 1/2$ ground-state doublet.

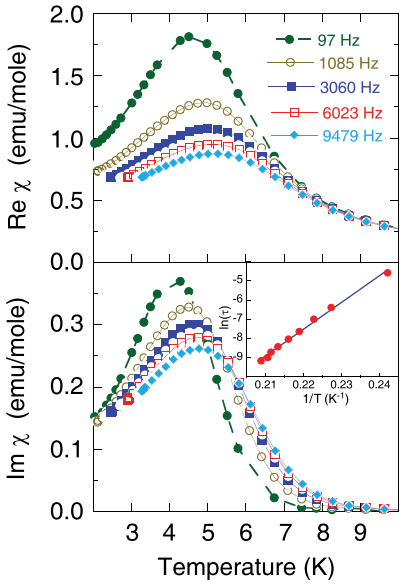

FIG. 4 (color online). Real (top panel) and imaginary (bottom panel) part components of the ac magnetic susceptibility as a function of temperature, measured at different frequencies f of the driving field. The natural logarithm of the relaxation time τ is plotted in the inset as function of $1/T$.

inductance technique. Data were collected on warming from 2 to 300 K after zero-field cooling of the sample. The driving field amplitude was 15 Oe, and the oscillation frequency varied between 97 and 10 000 Hz. With decreasing temperature below about 10 K, the in-phase and out-of-phase susceptibility components, $\mathrm{Re}\chi$ and $\mathrm{Im}\chi$, depend strongly on frequency, reflecting a marked slowing down of the dynamics that we attribute to superparamagnetic relaxation. Indeed, the shape of $\mathrm{Re}\chi$ is not cusplike as expected for spin-glass freezing. On the other hand, $\mathrm{Im}\chi$ shows a well-defined peak at a frequency-dependent temperature T_M where the relaxation time τ is equal to the characteristic measuring time $1/(2\pi f)$. Furthermore, this peak remains sharp and well-defined in the whole studied frequency range and $\mathrm{Im}\chi$ does not show any sign of low-temperature saturation at lower frequencies; this allows us to exclude the presence of any significant intermolecular interactions [16], so that the slow relaxation behavior is indeed of molecular origin. As shown in the inset of Fig. 4, $\tau(T)$ follows an exponential law, $\tau = \tau_0 \exp(U/k_B T)$, indicating that the main relaxation channel is a thermally activated Orbach process [11] with an effective energy barrier $U = 140$ K, a value comparable to that observed for rare-earth based single-ion magnets [17] and considerably larger than in transition-metal clusters. We have verified that the presence of energy levels around 140 K is compatible with the observed Curie behavior if they correspond to the $J_z = \pm\frac{5}{2}$ doublet of the Np^{VI} ion.

In conclusion, the Np_3 cluster is the first studied example of a polymetallic transuranic complex displaying both slow relaxation of the magnetization and effective superexchange interactions between $5f$ centers. In marked contrast with $4f$ complexes, this cluster is heterovalent, which is a property possible for actinides but normally not for lanthanides. The superexchange interaction of 10.8 K is also much larger than typical exchange interactions found in $4f$-ion clusters. It was also inferred that the overall ligand field is much stronger than for typical rare-earth-based molecules, since in the latter case the full free-ion susceptibility value is usually recovered well below room temperature [18]. This can be attributed partly to the larger radial extent of the $5f$ with respect to the $4f$ wave functions [19] and partly to the presence of two oxygen ligands at very close distances around each neptunium. These results suggest that actinide-based single molecule magnets could be obtained, with particular reference to higher-nuclearity clusters, holding the promise of larger anisotropy energy barriers and novel magnetic effects related to the nonquenched orbital degrees of freedom.

The European Commission is gratefully acknowledged for financial support under the Project No. ACT-07-1 of the ACTINET Network of Excellence and in the frame of the program ''Training and Mobility of Researchers''.

*Current address: Lawrence Berkeley National Laboratory, Chemical Sciences Division, Actinide Chemistry Group, 1 Cyclotron Road MS 70A1150, Berkeley CA 94720-8175, USA.

†Roberto.Caciuffo@ec.europa.eu

‡Current address: Chemistry Division (C-IIAC), Los Alamos National Laboratory, Los Alamos NM 87545, USA.

[1] D. Gatteschi, R. Sessoli, and J. Villain, *Molecular Nanomagnets* (Oxford University Press, Oxford, 2006); L. Bogani and W. Wernsdorfer, Nature Mater. **7**, 179 (2008); M. N. Leuenberger and D. Loss, Nature (London) **410**, 789 (2001).

[2] R. Sessoli *et al.*, Nature (London) **365**, 141 (1993); D. Gatteschi *et al.*, Science **265**, 1054 (1994).

[3] N. Ishikawa, M. Sugita, and W. Wernsdorfer, J. Am. Chem. Soc. **127**, 3650 (2005); Angew. Chem., Int. Ed. **44**, 2931 (2005).

[4] G. H. Lander, Science **301**, 1057 (2003).

[5] J. D. Rinehart and J. R. Long, J. Am. Chem. Soc. **131**, 12 558 (2009).

[6] R. K. Rosen, R. A. Andersen, and N. M. Edelstein, J. Am. Chem. Soc. **112**, 4588 (1990).

[7] J. D. Rinehart *et al.*, Inorg. Chem. **48**, 3382 (2009).

[8] S. A. Kozimor *et al.*, J. Am. Chem. Soc. **129**, 10 672 (2007).

[9] S. M. Cornet *et al.*, Chem. Commun. (Cambridge) 917 (2009).

[10] D. Newman and B. Ng, *Crystal Field Handbook* (Cambridge University Press, Cambridge, England, 2000).

[11] A. Abragam and B. Bleaney, *Electron Paramagnetic Resonance of Transition Ions* (Clarendon, Oxford, 1970).

[12] J. Mulak and M. Mulak, J. Phys. A **38**, 6081 (2005).

[13] J. Luzon *et al.*, Phys. Rev. Lett. **100**, 247205 (2008); K. Bernot *et al.*, J. Am. Chem. Soc. **131**, 5573 (2009).

[14] K. W. H. Stevens, Proc. Phys. Soc. London Sect. A **65**, 209 (1952).

[15] From the magnetic measurements one can estimate that the $J_z = \pm 3$ states are well isolated from the rest of the multiplet, so the only nonaxial ligand-field parameter which remains effective is B_6^6 (since O_6^6 is the only Stevens operator which has a nonzero matrix element between these two states). We have verified that adding a $B_6^6 = 10^{-3}$ K does not significantly change the fit of the superexchange constants. Using twice this value the calculated curves are still qualitatively compatible with the experimental data, but B_6^6 cannot be significantly larger. We conclude that this contribution must be at least 2 orders of magnitude smaller than the whole splitting due to the three axial ligand-field terms.

[16] N. Ishikawa *et al.*, J. Am. Chem. Soc. **125**, 8694 (2003).

[17] N. Ishikawa *et al.*, J. Phys. Chem. B **108**, 11 265 (2004).

[18] M. L. Kahn *et al.*, Chem. Eur. J. **8**, 525 (2002).

[19] J. P. Desclaux and A. J. Freeman, J. Magn. Magn. Mater. **8**, 119 (1978); A. J. Freeman and J. P. Desclaux, J. Magn. Magn. Mater. **12**, 11 (1979).